

# Application of the Min-Projection and the Model Predictive Strategies for Current Control of Three-Phase Grid-Connected Converters: A Comparative Study

M. Oloumi\_Baygi\*, R. Ghazi\*(C.A.) and M. Monfared\*

**Abstract:** This paper provides a detailed comparative study concerning the performance of Min-Projection Strategy (MPS) and Model Predictive Control (MPC) systems to control the three-phase grid connected converters. The MPS approach is already applied in synchronous reference frame by authors. However in this paper the algorithm is modified to be realized in the stationary reference frame which brings considerable simplicity and ease of implementation and then the MPS is compared with MPC. To do so, first, the converter is modeled as a switched linear system. Then, the feasibility of the MPS technique is investigated and its stability criterion is derived as a lower limit on the DC link voltage. The mathematical analysis reveals that the MPS is independent of the load, grid, filter and converter parameters. This feature is a great advantage of MPS over the MPC approach. However, the MPC is a mature model-based control technique, which has been already developed for controlling the VSC in the stationary reference frame. For comparing, both MPS and MPC approaches are simulated in the PSCAD/EMTDC environment. Simulation results illustrate that the MPS works well and is less sensitive to grid and filter inductances as well as the DC link voltage level. However, the MPC approach offers slightly a better performance in the steady state conditions.

**Keywords:** Grid-Connected Converter, Min-Projection Strategy (MPS), Model Predictive Control (MPC), Switched Linear System (SLS).

## 1 Introduction

With rapid expansion of different types of distributed generation systems that generate either DC or AC voltage with variable frequency, the Voltage Source Converters (VSCs) have come into increasing use as interfacing devices [1, 2]. A three-phase PWM-VSC is a commonly used topology in grid-connected applications to inject the regulated and high quality power from a DC source to the AC grid and vice versa. Hence, the current control of three-phase grid-connected VSCs has attracted the attention of many researchers over the past years.

Nonlinear techniques, such as the current hysteresis control [3-6], linear approaches, like the Proportional-Integral (PI) control [7], the Proportional-Resonant (PR) control [8], and hybrid controls are the well-known current control techniques, applied to VSCs [9, 10].

In the context of modeling, the average modeling is a common technique for the analysis and design of the control parameters for the linear and nonlinear current controllers. The hybrid modeling is another technique for analysis and control design of the power electronic converters [10]. The Switched Linear System (SLS) is an interesting class of the hybrid models with the capability of stability analysis and control of the complex nonlinear systems [11].

The power electronic converters are inherently switched linear systems with finite switching combinations; each can be represented by a single equation and for reaching to the equilibrium point, the best switching combination should be selected at the beginning of each time step. Model Predictive Control (MPC) [12] and Min-Projection Strategy (MPS) [13-16] are available techniques which can be employed for stabilization and control of the switched linear systems.

Simultaneous modeling of load, grid and converter is essential in the model predictive control technique. In this technique, behavior of the system variables is computed for all possible switching combinations for

Iranian Journal of Electrical & Electronic Engineering, 2015.

Paper first received 12 June 2014 and in revised form 18 Jan. 2015.

\* The Authors are with the Department of Electrical Engineering, Faculty of Engineering, Ferdowsi University of Mashhad.

E-mails: me\_oloomi@yahoo.com, rghazi@um.ac.ir and m.monfared@um.ac.ir.

the next switching period and the best one is selected to be applied to the VSC [17-20].

The simultaneous modeling of load, grid and converter is also necessary for implementing the MPS. In this method the best switching combination for the current control is selected by using the system states, model and the equilibrium point. In the MPS the best switching combination of the system is determined at each switching instant based on the stabilization of the system. For this purpose the influence of different switching combinations on the system stability is determined by computing the state variables from the state equations. Afterwards, the switching combination with the largest projection on the vector from the current system state to the equilibrium point is selected as the optimum switching combination. If at least one switching combination exists such that its projection is pointed towards the equilibrium point at each time, then the stability is guaranteed by the MPS [10, 13, 16].

Current control of the three-phase grid-connected converter using the MPS was introduced by the authors of the present paper in [16], where the mathematical analysis was conducted in the synchronous reference frame. In this paper the proposed strategy is modified to be implemented in the stationary reference frame. This approach provides considerable simplicity and ease of implementation.

The performance of MPS and MPC approaches in current control of three-phase grid-connected VSCs is thoroughly studied in this paper and the necessary comparisons are made. The rest of paper is organized as follows. The hybrid modeling of the VSC in the stationary reference frame is shown in Section 2. Sections 3 and 4 present the MPS and MPC algorithms. Sections 5, 6 and 7 present the SLS modeling of VSC, Stability analysis of MPS and control law base on the MPS respectively. Section 8 reports the simulation results and compares the performance of MPS and MPC, from different perspectives.

## 2 System Modeling

In this section, the state-space representation of a three-phase grid-connected VSC is derived in the stationary reference frame. Fig. 1 shows the power circuit of a three-phase full bridge grid-connected VSC with IGBT switches and an inductive filter.

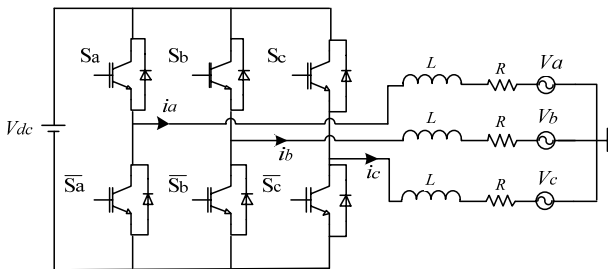


Fig. 1 Grid-connected three-phase VSC.

In this figure,  $V_{dc}$  is the dc-link voltage,  $i_a$ ,  $i_b$  and  $i_c$  represent the injected currents,  $R$  and  $L$  are resistance and inductance of the filter, respectively and  $V_a$ ,  $V_b$  and  $V_c$  denote the grid voltages.

The switching function  $p_j$ , which represents the switching status of each independent switch (each leg contains a dependent switch), is defined as

$$p_j = \begin{cases} 1 & S_j = \text{close} \\ 0 & S_j = \text{open} \end{cases} \quad j = a, b, c \quad (1)$$

The state-space equation of the system including the RL filter, the converter output voltage and the grid voltage can be expressed as:

$$L \frac{di}{dt} = -Ri + V_i - V \quad (2)$$

where,  $i = [i_a \ i_b \ i_c]^T$  and  $V = [V_a \ V_b \ V_c]^T$  are the injected currents and grid voltages, respectively, and  $V_i$  is the converter output voltage.  $V_{dc}$ ,  $V_i$  and  $p_i$  can be related by [21].

$$V_i = \frac{V_{dc}}{3} \begin{bmatrix} 2 & -1 & -1 \\ -1 & 2 & -1 \\ -1 & -1 & 2 \end{bmatrix} p_\sigma \quad (3)$$

where,  $\sigma$  is the switching combination and accepts a value within 0 to 7. For this system,  $p_\sigma = [p_{a\sigma} \ p_{b\sigma} \ p_{c\sigma}]^T$  is the switching function. By substituting Eq. (3) into Eq. (2) and then transforming the results into the stationary reference frame, the Eq. (2) can be re-stated as,

$$\frac{d}{dt} i_{\alpha\beta} = -\frac{R}{L} i_{\alpha\beta} + \frac{V_{dc}}{L} T p_\sigma + V_{\alpha\beta} \quad (4)$$

$$i_{\alpha\beta} = \begin{bmatrix} i_\alpha & i_\beta \end{bmatrix}^T = Ti \quad (5)$$

$$V_{\alpha\beta} = \begin{bmatrix} V_\alpha & V_\beta \end{bmatrix}^T = TV \quad (6)$$

$$T = \sqrt{\frac{2}{3}} \begin{bmatrix} 1 & -1/2 & -1/2 \\ 0 & -\sqrt{3}/2 & \sqrt{3}/2 \end{bmatrix} \quad (7)$$

where  $i_{\alpha\beta}$  and  $V_{\alpha\beta}$  indicate the injected current and grid voltage in the stationary reference frame, respectively. Equation (4) can be used by MPS and MPC to control the injected current of the three-phase grid connected converter.

## 3 Min-Projection Strategy

The mathematical description and fundamental equations of the MPS for the control of a grid-connected three-phase VSC are presented in this section. For a switched system described by the state equation in the form of  $dx/dt = f_\sigma(x)$ , with  $n$  distinct subsystems and equilibrium point  $x_{ref}$ , the projection of the vector field  $f_\sigma(x)$  on the vector  $(x - x_{ref})$  is defined as

$$\Gamma_\sigma(x) = (x - x_{ref})^T f_\sigma(x) / \|x - x_{ref}\| \quad x \neq x_{ref} \quad (8)$$

If  $\Gamma_\sigma(x) < 0$ , then the states of the system converge towards the equilibrium point and a smaller value of  $\Gamma_\sigma(x)$  indicates a faster convergence.

Based on the norm definition,  $\|x - x_{ref}\|$  is always positive for nonzero vectors. Hence without the loss of generality, the constraint  $x \neq x_{ref}$  can be eliminated and Eq. (8) can be rewritten as:

$$\Gamma'_\sigma(x) = (x - x_{ref})^T f_\sigma(x) \quad (9)$$

Since vector  $\Gamma_\sigma(x)$  is proportional to  $\Gamma'_\sigma(x)$ , the projections of  $\Gamma_\sigma(x)$  and  $\Gamma'_\sigma(x)$  on the vector  $(x - x_{ref})$  are not identical, but their corresponding vectors are proportional. Hence,  $\Gamma'_\sigma(x)$  can be used instead of  $\Gamma_\sigma(x)$ .

For a state-space representation in the form of  $dx/dt=f_\sigma(x)$ , finding the minimum value of the vector field  $\Gamma'_\sigma(x)$  and applying this vector to the system is a control technique known as the min-projection strategy or MPS [13]. According to this technique, the best strategy would be

$$\begin{aligned} \sigma_o(x) &= \arg \min_{\sigma \in \{1,2,\dots,n\}} (x - x_{ref})^T P f_\sigma(x) \\ &= \arg \min_{\sigma \in \{1,2,\dots,n\}} Q_\sigma \end{aligned} \quad (10)$$

where  $P$  is a positive definite matrix, representing the weights of the state variables. The whole procedure is described by the author of the present paper in [16].

#### 4 Model Predictive Control

The description of MPC for controlling of a grid-connected three-phase VSC is presented in this section. The performance of the MPC can be explained by referring to Fig. 2. In this figure,  $T_s$  and  $x(t_k)$  are sampling periods and the sampled state variables of a system with a finite number of switching combinations, respectively.

Each switching combination is used to predict the state variable at  $t_{k+1} = t_k + T_s$  as:

$$x_\sigma(t_{k+1}) = x(t_k) + T_s f_\sigma(x(t_k)) \quad (11)$$

A cost function is needed to determine the best switching combination, which is defined as:

$$Q_\sigma = g(x_{ref}(t_{k+1}), x_\sigma(t_{k+1})) \quad (12)$$

A typical example for cost function would be the absolute error between the predicted state and the reference, expressed below:

$$Q_\sigma = |x_{ref}(t_{k+1}) - x_\sigma(t_{k+1})| \quad (13)$$

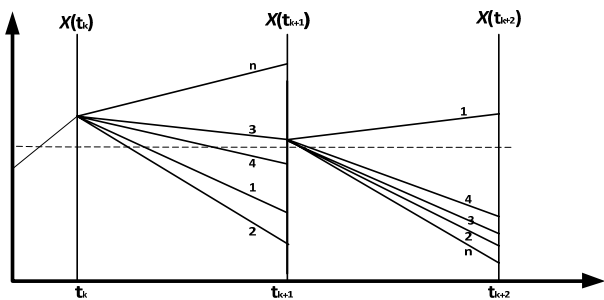


Fig. 2 Operation principle of MPC.

Selecting the best switching combination is mathematically stated by,

$$\sigma_o(x(t_k)) = \arg \min_{\sigma \in \{0,1,\dots,n-1\}} Q_\sigma \quad (14)$$

Hence, the switching combination corresponding to the minimum cost function is selected as the best switching combination to control the system.

The simplest form of MPC for controlling the current of VSCs is only based on the minimization of error between the reference and predicted line currents of the VSC, shown in Fig. 2. To do this, the state-space Eq. (4) is used and the predicted value of injected current is calculated from,

$$i_{\sigma,\alpha\beta}(t_{k+1}) = i_{\alpha\beta}(t_k) - \frac{T_s R}{L} i_{\alpha\beta}(t_k) + \frac{T_s V_{dc}}{L} T p_\sigma + T_s V_{\alpha\beta}(t_k) \quad (15)$$

Actual values of the injected current and grid voltage are measured and used by the predictive model to generate eight predictions of future current for each switching combination. These predictions are evaluated with a cost function  $Q_\sigma$  that is defined in Eq. (16) and the switching combination that minimizes this function is applied during the next switching interval.

$$Q_\sigma = |i_{ref,\alpha}(t_{k+1}) - i_{\sigma,\alpha}(t_{k+1})| + |i_{ref,\beta}(t_{k+1}) - i_{\sigma,\beta}(t_{k+1})| \quad (16)$$

#### 5 SLS Modeling of VSC

In this section, the procedure of deriving the hybrid model for a three-phase grid-connected VSC in the stationary reference frame is described. To do this, the state equation of VSC expressed by Eq. (4) is simplified as:

$$\frac{d}{dt} i_{\alpha\beta} = -\frac{R}{L} i_{\alpha\beta} + \frac{V_{dc}}{L} p_{\alpha\beta\sigma} + V_{\alpha\beta} \quad (17)$$

where,

$$p_{\alpha\beta\sigma} = [p_{\alpha\sigma} \quad p_{\beta\sigma}]^T = T p_\sigma \quad (18)$$

Switching function  $p_{\alpha\beta\sigma}$  in the stationary reference frame has been calculated and presented in Table 1.

Equation (17) can be expressed in the following linear state space form

$$\dot{x} = Ax + B_\sigma \quad (19)$$

Table 1 Switching function in the stationary reference frame.

$\sigma$	$p_a$	$p_b$	$p_c$	$p_{a\sigma}$	$p_{\beta\sigma}$
0	0	0	0	0	0
1	1	0	0	$\sqrt{2/3}$	0
2	0	1	0	$-\sqrt{6}/6$	$\sqrt{2}/2$
3	1	1	0	$\sqrt{6}/6$	$\sqrt{2}/2$
4	0	0	1	$-\sqrt{6}/6$	$-\sqrt{2}/2$
5	1	0	1	$\sqrt{6}/6$	$-\sqrt{2}/2$
6	0	1	1	$-\sqrt{2/3}$	0
7	1	1	1	0	0

where  $x=[i_\alpha \ i_\beta]^T$  is the state variable and  $A$  and  $B_\sigma$  are defined as:

$$A = -\frac{R}{L} \begin{bmatrix} 1 & 0 \\ 0 & 1 \end{bmatrix} \quad (20)$$

$$B_\sigma = \frac{V_{dc}}{L} p_{\alpha\beta\sigma} + V_{\alpha\beta} \quad (21)$$

The hybrid model of a three-phase grid-connected converter is described by Eqs. (19)-(21) and can be used for stability analysis and controller design of the VSC.

## 6 Stability Analysis of MPS

In order to apply the MPS method as a current controller for the grid-connected converter shown in Fig. 1, the stability assessment is necessary. For this purpose, the current reference or equilibrium point is defined as:

$$x_{ref} = \begin{bmatrix} i_{\alpha,ref} \\ i_{\beta,ref} \end{bmatrix} \quad (22)$$

where,  $i_{\alpha,ref}$  and  $i_{\beta,ref}$  denote the reference currents in the stationary reference frame. By setting the origin as the equilibrium point, i.e.  $x_{ref} = 0$ , then Eq. (19) can be rewritten as:

$$\dot{x} = A'x + B'_\sigma \quad (23)$$

where  $A' = A$  and  $B'_\sigma$  is defined as

$$B'_\sigma = Ax_{ref} + B_\sigma = Ax_{ref} + \frac{V_{dc}}{L} p_{\alpha\beta\sigma} + V_{\alpha\beta} \quad (24)$$

In Eq. (24),  $x_{ref}$  is the equilibrium point that is defined by Eq. (22). Stability of Eq. (23) can be analyzed using the following theorem.

**Theorem 1.** If there exist constants  $0 \leq \alpha_i \leq 1$  such that  $\alpha_0 + \alpha_1 + \dots + \alpha_7 = 1$ ,  $A_{eq}$  defined by Eq. (25) is Hurwitz and  $B_{eq}$  defined by Eq. (26) is zero ( $B_{eq} = 0$ ), then the MPS can quadratically stabilize the switched system with  $n$  distinct switching combinations [12, 14].

$$A_{eq} = \sum_{\sigma=0}^{n-1} \alpha_\sigma A_\sigma \quad (25)$$

$$B_{eq} = \sum_{\sigma=0}^{n-1} \alpha_\sigma B_\sigma \quad (26)$$

Substituting Eq. (20) into Eq. (25) yields:

$$A_{eq} = -\frac{R}{L} \begin{bmatrix} 1 & 0 \\ 0 & 1 \end{bmatrix} \quad (27)$$

Obviously, the eigenvalues of Eq. (27) are located at left hand side of the  $s$ -plane for every value of  $R$  and  $L$ ; indicating  $A_{eq}$  is a Hurwitz matrix.

Substituting Eq. (24) into Eq. (26) gives

$$p_\alpha^* = \sum_{\sigma=0}^7 \alpha_\sigma p_{\alpha\sigma} = \frac{1}{V_{dc}} (Ri_{\alpha,ref} + V_\alpha) \quad (28)$$

$$p_\beta^* = \sum_{\sigma=0}^7 \alpha_\sigma p_{\beta\sigma} = \frac{1}{V_{dc}} (Ri_{\beta,ref} + V_\beta) \quad (29)$$

where  $p_\alpha^*$  and  $p_\beta^*$  are defined as auxiliary variables. Equation (30) presents the necessary condition for existing at least one convex combination of the switch functions such that Eq. (28) and Eq. (29) are satisfied. The mathematical proof is presented in the Appendix.

$$p_\alpha^{*2} + p_\beta^{*2} \leq 0.6667 \quad (30)$$

Substituting Eq. (28) and Eq. (29) into Eq. (30), results in:

$$R^2 (i_{\alpha,ref}^2 + i_{\beta,ref}^2) + (V_\alpha^2 + V_\beta^2) + 2RV_\alpha i_{\alpha,ref} - 2RV_\beta i_{\beta,ref} \leq 0.6667V_{dc}^2 \quad (31)$$

Equation (31) represents the stability condition for the MPS controller as a lower limit on the DC link voltage.

## 7 Control Law Based on the MPS

In this section a control law based on the MPS is derived. In the MPS technique, the state variables can be weighted by choosing a proper  $P$ . The grid-connected converter shown in Fig. 1, contains only one state variable. Hence, for eliminating  $L$  from the calculations,  $P$  is set to  $diag[L \ L]$ , which is a positive definite matrix. By substituting  $P$  into the state equation of the converter,  $Q_\sigma(x)$  from Eq. (10) can be restated as

$$Q_\sigma(x) = (x - x_{ref})^T diag [L \ L] (Ax + B_\sigma) \quad (32)$$

Equation (32) can be expressed as.

$$Q_\sigma(x) = -Ri_\alpha^2 + V_{dc}i_\alpha p_{\alpha\sigma} + Ri_\alpha i_{\alpha,ref} - V_{dc}i_{\alpha,ref} p_{\alpha\sigma} - Ri_\beta^2 + V_{dc}i_\beta p_{\beta\sigma} + Ri_\beta i_{\beta,ref} - V_{dc}i_{\beta,ref} p_{\beta\sigma} \quad (33)$$

In Eq. (33), there are several terms which are not functions of  $\sigma$ . These terms do not have any effect on  $\sigma_0$ . Hence, they can be removed from  $Q_\sigma(x)$ , and accordingly Eq. (33) can be simplified to:

$$Q_\sigma(x) = (i_\alpha - i_{\alpha,ref})p_{\alpha\sigma} + (i_\beta - i_{\beta,ref})p_{\beta\sigma} \quad (34)$$

According to Eq. (34), the suggested control technique does not require any information about the filter parameters and the DC-link voltage.

## 8 Simulation Results

To compare the performance of the MPS and MPC, the three-phase grid-connected VSC is simulated in PSCAD/EMTDC environment. The circuit diagram of the simulated converter is shown in Fig. 1 and the system parameters are listed in Table 2.

The block diagram of MPS and MPC are illustrated in Fig. 3. According to these block diagrams, only the grid voltage and current in the stationary reference frame and the references for active and reactive powers are used to calculate the best switching combination in the MPS controller. In the MPC controller, resistance ( $R$ ) and inductance ( $L$ ) of the filter, sampling frequency ( $f_{sa}$ ) and the voltage of DC link ( $V_{dc}$ ), in addition to the grid voltage and current, are used to calculate the best switching combination.

**Table 2** Parameters of the grid-connected converter.

symbol	Parameter	Value	Unit
$R$	filter resistance	200	mΩ
$L$	filter inductance	10	mH
$V_{dc}$	DC-link voltage	150	V
$f$	grid frequency	50	Hz
$V_n$	grid voltage	$50\sqrt{3}$	V
$f_{sa}$	sampling frequency	15	kHz

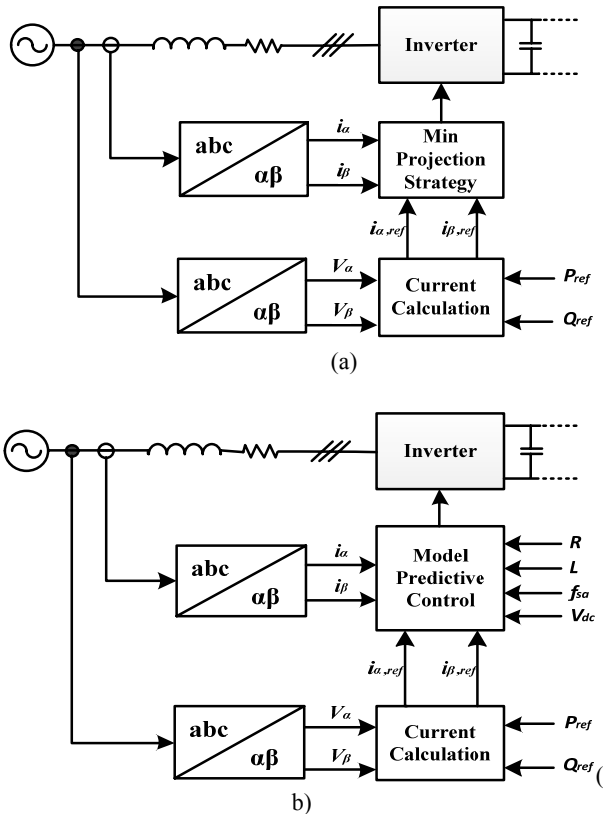


**Fig. 3** The block diagram of (a) MPS and (b) MPC.

In order to compare the performance of MPS and MPC, extensive simulations have been carried out. The steady-state performance, presented in Fig. 4, shows that the filter current and active and reactive powers in MPS and MPC are almost similar. The harmonic spectrum of the three-phase grid-connected converter controlled by MPS and MPC at steady-state condition are presented in Fig. 5. These results indicate that the harmonic spectrum of MPS mainly lies at the low frequency range, and the MPC provides slightly better low order harmonics performance. The THD of MPS and MPC are 2.76 % and 2.17 %, respectively.

The transient waveforms in response to step changes of power references are presented in Fig. 6. Based on the illustrated results, MPS and MPC show almost similar transient performance. Indeed, following a step change, both techniques can provide fast and smooth transient performance with decoupled control of active and reactive powers.

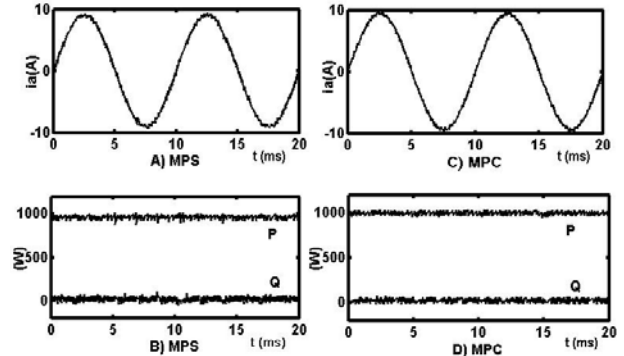


**Fig. 4** Steady-state performance of MPS and MPC.

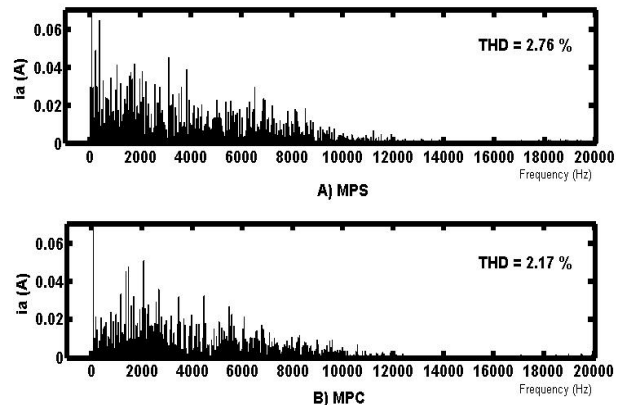


**Fig. 5** Harmonic spectrum of MPS and MPC.

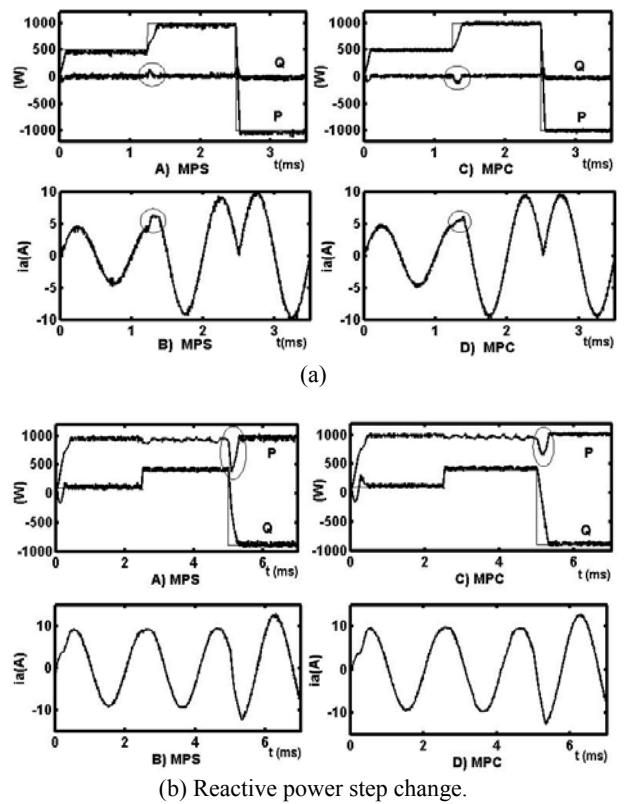


**Fig. 6** Transient response of MPS and MPC. (a) Active power step change (b) Reactive power step change

The sensitivity of the current and power control efficiency to the changes of grid inductance for the MPS and MPC are presented in Fig. 7. The results of Fig. 7 show that the MPC is quite sensitive to the grid inductance value. If the grid inductance increases to 0.15L, then the THD increases to 23.10 %.

However, the MPS is much less sensitive to the grid parameters. For instance, for a high value of grid inductance (0.5L), the THD of MPS is limited to 26.69 %, while the THD of MPC rises to 74.46 %. The sensitivity to the filter inductance mismatches is presented in Fig. 8. Also, Fig. 9 shows the sensitivity to the voltage level of the DC link.

The results demonstrate that the MPC is very sensitive to the filter inductance mismatch, especially if the value used for the filter inductance in the simulation is smaller than its real one; the performance of MPC is highly degraded. Also, the results show that the sensitivity of current and powers to the voltage level of the DC link of MPS is less than MPC.

The performance of the MPS and MPC with different sampling frequencies is presented in Table 3. In this table the power error is defined as

$$S_{error} [\%] = \sqrt{\frac{(P - P_{ref})^2 + (Q - Q_{ref})^2}{P_{ref}^2 + Q_{ref}^2}} \quad (35)$$

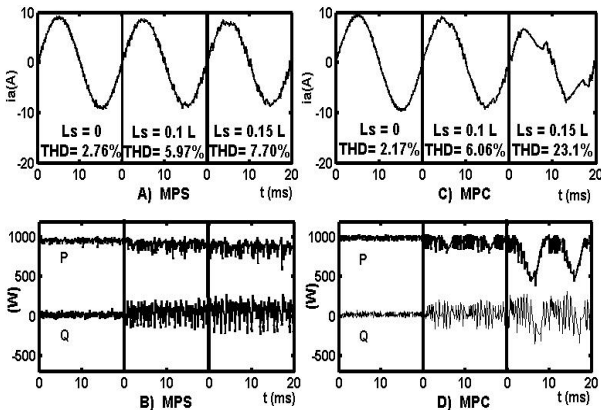


Fig. 7 Sensitivity to grid inductance of MPS and MPC.

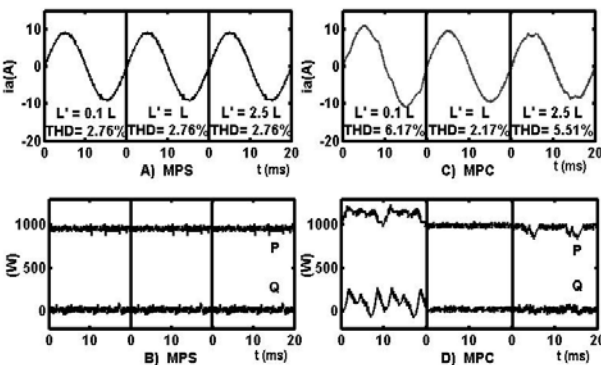


Fig. 8 Sensitivity to filter inductance mismatch of MPS and MPC.

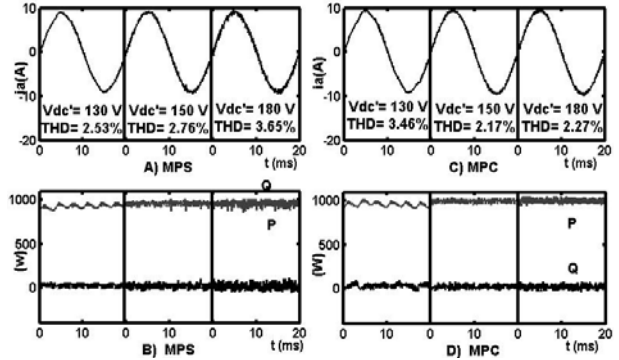


Fig. 9 Sensitivity to voltage of DC link of MPS and MPC.

Table 3 Sensitivity of MPS and MPC to sampling frequency.

		$f_{sa}(\text{Hz})$			
		5	10	15	20
THD (%)	MPS	9.47	4.21	2.77	2.14
	MPC	5.82	3.06	2.17	1.66
$S_{error}$ (%)	MPS	12.68	6.43	4.33	3.38
	MPC	6.43	3.33	2.23	1.69
ASF (Hz)	MPS	700	1650	2400	3150
	MPC	650	1250	2050	2100

Table 4 Sensitivity of MPS and MPC to imbalance conditions.

		$k(\%)$			
		0	1	3	5
THD (%)	MPS	2.76	3.32	6.59	9.69
	MPC	2.17	2.71	5.56	8.69
$S_{error}$ (%)	MPS	4.33	4.47	4.24	4.48
	MPC	2.23	2.33	2.21	2.26
ASF (Hz)	MPS	2100	2100	2100	2100
	MPC	2000	2000	2000	2000

According to the Table 3, the performance of the MPS and MPC will be improved with increasing the sampling frequency. Moreover, the performance of MPC in terms of Average Switching Frequency (ASF), THD value and power tracking is slightly better than the MPS.

Table 4 compares the performance of MPS and MPC under imbalanced voltage condition, which is defined as:

$$\begin{aligned} V_a &= V_p \sin(\omega t) + kV_p \sin(\omega t) \\ V_b &= V_p \sin(\omega t - \frac{2\pi}{3}) + kV_p \sin(\omega t + \frac{2\pi}{3}) \\ V_c &= V_p \sin(\omega t + \frac{2\pi}{3}) + kV_p \sin(\omega t - \frac{2\pi}{3}) \end{aligned} \quad (36)$$

where  $V_p$  is the peak value of phase grid voltage and  $k$  denotes the percentage of imbalance. The performance of the MPS and MPC is evaluated for different values of  $k$ . The obtained results show that both MPS and MPC render a deteriorated performance as the level of imbalance increases.

Table 5 compares the performance of MPS and MPC when the grid voltage is distorted by the 5<sup>th</sup> and 7<sup>th</sup> harmonics, defined by:

$$\begin{aligned} V_a &= V_p \sin(\omega t) + k_5 V_p \sin 5(\omega t) + k_7 V_p \sin 7(\omega t) \\ V_b &= V_p \sin(\omega t - \frac{2\pi}{3}) + k_5 V_p \sin 5(\omega t - \frac{2\pi}{3}) \\ &\quad + k_7 V_p \sin 7(\omega t - \frac{2\pi}{3}) \\ V_c &= V_p \sin(\omega t + \frac{2\pi}{3}) + k_5 V_p \sin 5(\omega t + \frac{2\pi}{3}) \\ &\quad + k_7 V_p \sin 7(\omega t + \frac{2\pi}{3}) \end{aligned} \quad (37)$$

where  $k_5$  and  $k_7$  are the percentage of 5<sup>th</sup> and 7<sup>th</sup> harmonics, respectively. The performance of the MPS and MPC is evaluated for different values of  $k_5$  and  $k_7$ . The results show that both MPS and MPC have similar trends.

The results of above comparative evaluations are summarized in Table 6, regarding their individual advantages and disadvantages.

**Table 5** Sensitivity of MPS and MPC to harmonics polluting.

		$k_5=0\%$	$k_5=1\%$	$k_5=3\%$	$k_5=5\%$
		$k_7=0\%$	$k_7=1\%$	$k_7=3\%$	$k_7=5\%$
THD (%)	MPS	2.76	3.83	8.36	12.84
	MPC	2.16	3.37	7.44	12.43
Serror (%)	MPS	4.33	4.22	4.71	6.77
	MPC	2.23	2.25	2.56	3.89
ASF (Hz)	MPS	1900	1900	1900	1900
	MPC	1850	1850	1850	1850

**Table 6** Performance features of MPS and MPC.

Feature	MPS	MPC
Computational burden	Low	High
Algorithm complexity	Low	Moderate
Sensitivity to system parameters	Negligible	High
Current THD (%)	2.76	2.16
Transient response	Fast	Fast
Coupling between active and reactive powers	Low	Low
Sensitivity to grid inductance	Low	High
Sensitivity to filter inductance mismatch	Negligible	High
Sensitivity to DC link voltage level	Low	Low
Average switching frequency	Low	Low
Sensitivity to imbalance conditions	High	Relatively high
Sensitivity to harmonic pollution	High	Relatively high

## 9 Conclusion

In this paper, the Min Projection Strategy (MPS) is employed for current control of a three-phase grid-connected VSC in stationary references frame rather

than the synchronous one. Its performance is thoroughly compared with the well-known Model Predictive Control (MPC) approach. The MPS approach is implemented on a three-phase grid-connected converter which is modeled as a hybrid system using the concept of switched linear system considering the stability criteria. The MPC approach is also implemented. The comparative assessments are carried out for different operating conditions. These conditions include their steady state and transient performance due to step change in active and reactive powers, sensitivity to grid inductance, filter inductance, DC link voltage, sampling frequency, the grid voltage distortion and unbalances. The results show that both controllers doing well at normal condition, but the performance of MPC is slightly better than the MPS. This is expected as the MPC uses a lot of information about the system than the MPS. Based on the obtained results the MPS is much less sensitive to the grid inductance, filter inductance mismatch and the DC link voltage level. Being less sensitive to system parameters and the requirement of lower system information are the suitability of MPS method. The advantages and disadvantages are summarized and reported in this paper.

## Appendix

To prove the stability of a switched linear system in the form of Eq. (19), existence of convex combination solution for Eq. (28) and Eq. (29) is essential. For finding the necessary and sufficient condition, Eq. (28) and Eq. (29) are restated as,

$$\begin{cases} \sum_{\sigma=0}^7 \alpha_{\sigma} p_{\alpha\sigma} = p_{\alpha}^* \\ \sum_{i=0}^7 \alpha_{\sigma} p_{\beta\sigma} = p_{\beta}^* \end{cases} \quad (A1)$$

By substituting  $p_{\alpha\sigma}$  and  $p_{\beta\sigma}$  from Table 1, the result of these equations can be stated as,

$$\begin{cases} \alpha_1 = 0.5\sqrt{6}p_{\alpha}^* + 0.5\sqrt{2}p_{\beta}^* - \alpha_3 + \alpha_4 + \alpha_6 \\ \alpha_2 = \sqrt{2}p_{\beta}^* - \alpha_3 + \alpha_4 + \alpha_5 \end{cases} \quad (A2)$$

To guarantee the convex combination solution, i.e.  $\alpha_0 + \alpha_1 + \dots + \alpha_7 = 1$  and  $0 \leq \alpha_i \leq 1$ , it is necessary to limit  $(p_{\alpha}^{*2} + p_{\beta}^{*2})^{0.5}$ , or finding the maximum value of  $(p_{\alpha}^{*2} + p_{\beta}^{*2})^{0.5}$  subject to the convex combination conditions. Hence it is necessary to solve the following optimization problem.

$$\begin{aligned} & \text{Max } \sqrt{p_{\alpha}^{*2} + p_{\beta}^{*2}} \text{ subject to} \\ & \sum_{i=0}^7 \alpha_i = 1 \\ & 0 \leq \alpha_1 = 0.5\sqrt{6}p_{\alpha}^* + 0.5\sqrt{2}p_{\beta}^* - \alpha_3 + \alpha_4 + \alpha_6 \leq 1 \\ & 0 \leq \alpha_2 = \sqrt{2}p_{\beta}^* - \alpha_3 + \alpha_4 + \alpha_5 \leq 1 \\ & 0 \leq \alpha_0 \leq 1, 0 \leq \alpha_3 \leq 1, 0 \leq \alpha_4 \leq 1 \\ & 0 \leq \alpha_5 \leq 1, 0 \leq \alpha_6 \leq 1, 0 \leq \alpha_7 \leq 1 \end{aligned} \quad (A3)$$

For simplicity, the quadprog function in Matlab is used to solve this problem. For this purpose, Eq. (A3) should be written in the following standard form:

$$\begin{aligned} & \text{Min } -.5(p_{\alpha}^{*2} + p_{\beta}^{*2}) \text{ subject to} \\ & \alpha_0 + 0.5\sqrt{6}p_{\alpha}^* + 1.5\sqrt{2}p_{\beta}^* \\ & -\alpha_3 + 3\alpha_4 + 2\alpha_5 + 2\alpha_6 + \alpha_7 = 1 \\ & 0.5\sqrt{6}p_{\alpha}^* + 0.5\sqrt{2}p_{\beta}^* - \alpha_3 + \alpha_4 + \alpha_6 \leq 1 \\ & -(0.5\sqrt{6}p_{\alpha}^* + 0.5\sqrt{2}p_{\beta}^* - \alpha_3 + \alpha_4 + \alpha_6) \leq 0 \\ & \sqrt{2}p_{\beta}^* - \alpha_3 + \alpha_4 + \alpha_5 \leq 1 \\ & -(\sqrt{2}p_{\beta}^* - \alpha_3 + \alpha_4 + \alpha_5) \leq 0 \\ & 0 \leq \alpha_0 \leq 1, 0 \leq \alpha_3 \leq 1, 0 \leq \alpha_4 \leq 1 \\ & 0 \leq \alpha_5 \leq 1, 0 \leq \alpha_6 \leq 1, 0 \leq \alpha_7 \leq 1 \end{aligned} \quad (\text{A4})$$

The quadprog function can be used as,

$$\alpha^* = \text{quadprog}(H, f, A, b, A_{eq}, b_{eq}, lb, ub, x_0, Option) \quad (\text{A5})$$

where

$$\begin{aligned} \alpha^* &= [\alpha_0 \quad p_{\alpha}^* \quad p_{\beta}^* \quad \alpha_3 \quad \alpha_4 \quad \alpha_5 \quad \alpha_6 \quad \alpha_7] \\ H &= \begin{bmatrix} 0 & 0 & 0 & 0 & 0 & 0 & 0 & 0 \\ 0 & 1 & 0 & 0 & 0 & 0 & 0 & 0 \\ 0 & 0 & 1 & 0 & 0 & 0 & 0 & 0 \\ 0 & 0 & 0 & 0 & 0 & 0 & 0 & 0 \\ 0 & 0 & 0 & 0 & 0 & 0 & 0 & 0 \\ 0 & 0 & 0 & 0 & 0 & 0 & 0 & 0 \\ 0 & 0 & 0 & 0 & 0 & 0 & 0 & 0 \\ 0 & 0 & 0 & 0 & 0 & 0 & 0 & 0 \end{bmatrix} \\ f &= [0 \quad 0 \quad 0 \quad 0 \quad 0 \quad 0 \quad 0 \quad 0] \\ A &= \begin{bmatrix} 0 & 0.5\sqrt{6} & 0.5\sqrt{2} & -1 & 1 & 0 & 1 & 0 \\ 0 & 0 & \sqrt{2} & -1 & 1 & 1 & 0 & 0 \\ 0 & -0.5\sqrt{6} & -0.5\sqrt{2} & 1 & -1 & 0 & -1 & 0 \\ 0 & 0 & -\sqrt{2} & 1 & -1 & -1 & 0 & 0 \end{bmatrix} \\ b &= [1 \quad 1 \quad 0 \quad 0]^T \\ A_{eq} &= [1 \quad 0.5\sqrt{6} \quad 1.5\sqrt{2} \quad -1 \quad 3 \quad 2 \quad 2 \quad 1] \\ b_{eq} &= 1 \\ lb &= [0 \quad -100 \quad -100 \quad 0 \quad 0 \quad 0 \quad 0 \quad 0] \\ ub &= [1 \quad 100 \quad 100 \quad 1 \quad 1 \quad 1 \quad 1 \quad 1] \end{aligned} \quad (\text{A6})$$

The results of this optimization show that the maximum value of  $p_{\alpha}^{*2} + p_{\beta}^{*2}$  is 0.6667, that is:

$$p_{\alpha}^{*2} + p_{\beta}^{*2} \leq 0.6667 \quad (\text{A7})$$

## References

- [1] A. Khajeh and R. Ghazi, "GA-Based Optimal LQR Controller to Improve LVRT Capability of DFIG Wind Turbines", *Iranian Journal of Electrical & Electronic Engineering*, Vol. 9, No. 3, pp. 167-176, Sep. 2013.
- [2] R. Noroozian, M. Abedi, G. B. Gharehpetian and S. H. Hosseini, "Operation of Stand Alone PV Generating System for Supplying Unbalanced AC Loads", *Iranian Journal of Electrical & Electronic Eng.*, Vol. 3, No. 3 & 4, pp. 98-115, July 2007.
- [3] M. Lafoz, L. J. Iglesias, S. Portillo and D. Ugena, "Experimental results of a three-level voltage source inverter with hysteresis-band current control and hybrid PWM-SVM voltage control", in *Proc. Conf. Record Power Electronics Specialists, Mexico*, pp. 1703-1708, June 15-19, 2003.
- [4] K. Chaniago, J. Selvaraj and N. A. Rahim, "implementation of hysteresis current control for single-phase grid connected inverter", *7-th Int. Conf. on Power Electronics and Drive Systems (PEDS)*, pp. 1097-1101, Nov. 27-30, 2007.
- [5] H. Mao, X. Yang, Z. Chen and Z. Wang, "A hysteresis current controller for single-phase three-level voltage source inverters", *IEEE Transaction on Power Electronics*, Vol. 27, No. 7, pp. 3330-3339, July 2012.
- [6] C. N. M. Ho, V. S. P. Cheung and H. S. H. Chung, "Constant frequency hysteresis current control of grid-connected VSI without bandwidth control", *IEEE transaction on power electronics*, Vol. 24, No. 11, pp. 2484-2495, Nov. 2009.
- [7] M. Monfared and S. Golestan, "Control strategies for single-phase grid integration of small-scale renewable energy sources: A review", *Renewable and Sustainable Energy Reviews*, Vol. 16, No. 7, pp. 4982-4993, Sep. 2012.
- [8] B. Bahrani, A. Rufer, S. Kenzelmann and L. A. C. Lopes, "Vector control of single-phase voltage-source converters based on fictive-axis emulation", *IEEE Transactions on Industrial Applications*, Vol. 47, No. 2, pp. 831-840, 2011.
- [9] S. Pettersson, "Analysis and design of hybrid systems", *Ph.D. Thesis, Department of Signals and Systems, Chalmers University of Technology, Goteborg, Sweden*, 1999.
- [10] M. Senesky, G. Eirea, and T. JohnKoo, *Hybrid modeling and control of power electronics*, Springer-Verlag, Berlin Heidelberg 2003.
- [11] H. Lin and P. J. Antsaklis, "Stability and stabilizability of switched linear systems: A survey of recent results", *IEEE Transaction on Automatic Control*, Vol. 54, No. 2, pp. 308-322, Feb. 2008.
- [12] M. Lazar, "Model predictive control of hybrid systems: stability and robustness", *Ph.D. Thesis, Eindhoven university of technology*, 2006.
- [13] S. Pettersson, and B. Lennartson, "Stabilization of hybrid systems using a min-projection strategy", *Proceedings of American Control Conference*, Vol. 1, pp. 223-228, VA. USA, June 2001.
- [14] W. Xiao, B. Zhang and D. Qiu, "Modeling and control rule of three-phase boost-type rectifier as switched linear systems", *Int. Conference on Electrical Machines and Systems, (ICEMS), Wuhan. China*, pp. 1849-1854, Oct. 2008.

- [15] X. Wang, Y. Tang, X. Zong and P. Wang, "Switched control of DC/DC converter based on hybrid model", *2nd International Conference on Information Engineering and Computer Science (ICIECS), Wuhan. China*, pp. 1-3, Dec. 2010.
- [16] M. Oloumi\_Baygi, R. Ghazi and M. Monfared, "Applying the min-projection strategy to improve the transient performance of the three-phase grid-connected inverters", *ISA Transactions*, Vol. 53, No. 4, pp. 1131-1142, July 2014.
- [17] J. Rodriguez, J. Pontt, P. Correa, P. Lezana and P. Cortes, "Predictive power control of an AC/DC/AC converter", in *Industry Applications Conference, Fortieth IAS Annual Meeting, Hong Kong*, pp. 934-939, Oct. 2005.
- [18] A. Nachiappan and V. Malarselvam, "Application of predictive current control to a voltage source inverter", in *Proc. IEEE-Int. Conf. On Advances In Engineering, Science And Management (ICAESM)*, pp. 496-501, March 2012.
- [19] P. Cortés, M. P. Kazmierkowski, R. M. Kennel, D.E. Quevedo, and José Rodríguez, "Predictive control in power electronics and drives", *IEEE Trans. Ind. Elec.*, Vol. 55, No. 12, pp. 4312-4324, Dec. 2008.
- [20] R. Kennel and A. Linder, "Predictive control of inverter supplied electric drives", in *Proc. Conf. Record Power Electronics Specialist, Galway, Ireland*, pp. 761-766, Jun. 2000.
- [21] A. N. Yazdani and R. Iravani, *Voltage source converter in power systems* Wiley-IEEE press, 2010.



**Mahdi Oloumi\_Baygi** Received the B.Sc. degree from Shahrood University of technology, Shahrood, Iran in 1999, and the M.Sc. degree from Ferdowsi University of Mashhad, Iran, in 2002 both in electrical engineering. He is currently working towards his Ph.D. degree in electrical engineering at Ferdowsi University of Mashhad, Iran.

His Research interests include power electronics, renewable energy system, energy management, and power system economics.



**Reza Ghazi** was born in Semnan, Iran in 1952. He received his B.Sc., degree (with honors) from Tehran University of Science and Technology, Tehran, Iran in 1976. In 1986 he received his M.Sc. degree from Manchester University, Institute of Science and Technology (UMIST) and the Ph.D. degree in 1989 from University of Salford UK, all in electrical engineering.

Following receipt of the Ph.D. degree, he joined the faculty of engineering Ferdowsi University of Mashhad, Iran as an Assistant Professor of electrical engineering. He is currently Professor of Electrical Engineering in Ferdowsi University of Mashhad, Iran. His main research interests are reactive power control, FACTS devices, application of power electronic in power systems, distributed generation (DG's), restructured power systems control and analysis. He has published over 100 papers in these fields including three books.



**Mohammad Monfared** (S'07-M'10) received the B.Sc. degree in electrical engineering from Ferdowsi University of Mashhad, Iran, in 2004, and the M.Sc. and Ph.D. degrees (both with honors) in electrical engineering from Amirkabir University of Technology, Tehran, Iran, in 2006 and 2010, respectively. He is currently an

Assistant Professor at Ferdowsi University of Mashhad, Iran. His research interests include power electronics, motor drives, renewable energy systems, energy conversion, and control and applications.